Nanomaterials

DOI: 10.1002/anie.201105217

Optical Imaging of CdSe Nanowires with Nanoscale Resolution**

*Miriam Böhmler, Zhe Wang, Anton Myalitsin, Alf Mews, and Achim Hartschuh**

Inorganic semiconducting nanowires (NWs) are promising candidates as building blocks in nanoscale optoelectronics, photovoltaics, and sensing devices owing to their unique physical properties.[1–3] In cadmium selenide (CdSe) NWs, diameter-dependent quantum confinement (QC) controls the electronic band gap energy, a key parameter in potential applications, as shown by photoluminescence (PL) spectroscopy.[4] In addition, the band gap energy is known to depend on the crystal phase, ranging from 1.797 eV for wurtzite (WZ) to 1.712 eV for zinc blende (ZB).[3,5] Nanoscale phase variations with alternating WZ and ZB segments along NWs have been suggested as the origin of the large spectral width of the observed PL bands.[6] Unfortunately, the resolution of conventional optical microscopy is limited by diffraction and only a few experiments on NWs in the quantum-confinement regime with sub-diffraction resolution have been performed.[7–10]

Herein we present PL and Raman investigations on CdSe NWs applying tip-enhanced near-field optical microscopy (TENOM) that reveal significant variations of the CdSe NWs optical properties on the nanoscale. TENOM provides enhanced detection sensitivity and a spatial resolution limited by the size of the near-field (NF) probe reaching down to 10 nm.[11] A schematic of the setup is shown in Figure 1 together with a high-resolution transmission electron microscopy (HRTEM) image of a typical sample structure.

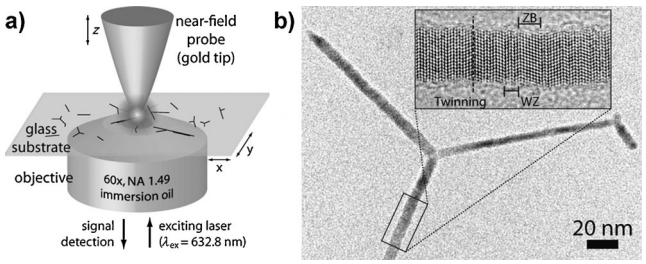

Figure 1. a) Schematic of the setup. b) TEM image of a branched CdSe NW. Inset: HRTEM image showing crystal phase variations.

[*] M. Böhmler, Prof. Dr. A. Hartschuh
Department Chemie and CeNS
Ludwig-Maximilians-Universität München
Butendtstraße 5–13 E, 81377 München (Germany)
E-mail: achim.hartschuh@cup.lmu.de
Homepage: http://www.cup.uni-muenchen.de/pc/hartschuh/
Z. Wang, A. Myalitsin, Prof. Dr. A. Mews
Department Chemie, Universität Hamburg
Grindelallee 117, 20146 Hamburg (Germany)

[**] We thank T. Dennenwaldt and Prof. C. Scheu for TEM measurements. Financial support was provided by the DFG through the Nanosystems Initiative Munich (NIM).

In Figure 2a a conventional far-field image of CdSe NWs detected by a photodiode after spectral filtering to extract the PL signal between 698 nm and 708 nm is shown. Figure 2b

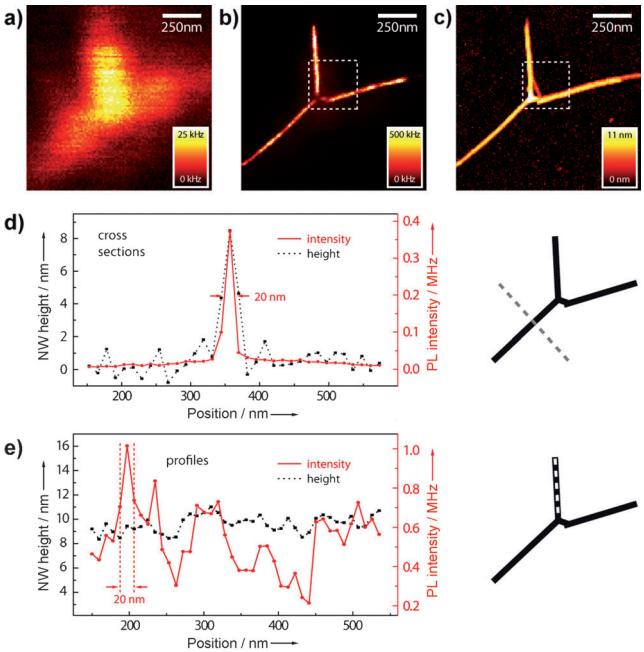

Figure 2. PL images of CdSe NWs on glass. a) Diffraction-limited confocal image. b) TENOM image of the same sample area as in (a). Local signal enhancement by the tip results in substantially improved resolution as shown by a cross section (d) and a profile (e) (measured along dashed lines indicated in the insets). c) Simultaneously detected topographic image.

presents the TENOM PL image of the same area, Figure 2c the simultaneously obtained topography. Tip-enhancement leads to a substantial increase of the PL intensity from about 25 kHz to 500 kHz. The resolution has improved from 240 nm to 20 nm as determined from cross sections as well as profiles along a NW (Figure 2d and e). The TENOM data reveal that the structure is of tripod shape where the right arm is broken close to the branching site (for information on branching mechanisms and nomenclature see Ref. [3]). While the NWs are found to be luminescent for their complete length, the PL intensity is seen to vary strongly within few tens of nanometers without significant changes in NW height (Figure 2e).

Surprisingly, the PL intensity fades toward the central branching site; the junction core itself is completely dark in an area about 30 nm long. In fact, all of the six branched NWs that we investigated featured this dark junction site. Literature HRTEM data indicate that the cores typically have pure ZB structure and could thus be expected to be luminescent.[12] ZB–WZ interfaces, in contrast, should result in type-II

transitions with reduced oscillator strength because of the partial charge transfer.[6] Modified optical properties could in principle result from the particular dimensionality of the core that could lead to different quantum-confined electronic states or an increased density of defect-related quenching sites.

The topographical image (Figure 2c) shows that additional thinner NWs are present in the scanned area that are hardly visible in the PL image, which only covered a limited spectral window. Hyperspectral imaging achieved by recording complete emission spectra at each image pixel provides detailed information beyond simple visualization. Figure 3 shows hyperspectral image data of the central region of the NW sample in Figure 2. Two example spectra of this measurement are depicted in Figure 3b taken at positions I and II marked in the topographical image obtained simultaneously (Figure 3a).

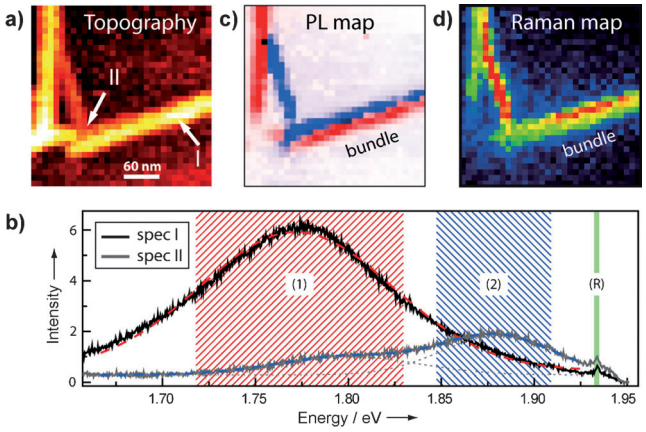

Figure 3. Hyperspectral imaging of the CdSe NWs (as marked in Figure 1b and c by the dashed boxes). a) Topographical image. b) Spectra taken at the positions marked in (a) show PL bands at around 1.772 eV (1) and 1.880 eV (2) that can be described by Gaussian line shape functions. A Raman band (R; LO phonon) is visible at 1.934 eV. c) Intensity maps of PL (1; red) and PL (2; blue) bands show higher PL energies for thinner NWs. d) The Raman map reveals stronger scattering for thinner NWs. In the hyperspectral image the two NWs forming the bundle are clearly resolved.

Spectrum I is dominated by a broad PL band at around 1.772 eV labeled (1), spectrum II features an additional band at around 1.880 eV labeled (2). In both spectra a Raman peak at 1.934 eV (206 cm^{-1}) is visible, which results from the longitudinal optical phonon mode.[13]

The contributions of the two PL bands were determined by fitting each spectrum with two Gaussian line shape functions. The resulting amplitude images were normalized and plotted in an intensity map (Figure 3c). Clearly, the low-energy PL band (1; red in Figure 3c) originates from the thicker three-armed CdSe nanostructure, whereas the thinner NWs show blue-shifted PL energy (PL band (2); blue). The increase of the band gap with decreasing diameter, a result of quantum confinement, is clearly visible. Notably, although the thin and thick NWs are bundled together and can hardly be distinguished from topography we can clearly resolve and localize them with TENOM based on their optical characteristics. The intensities of the thinner NWs are comparable and apparently independent of their distance from the thicker NWs. This implies that there is no efficient energy transfer from the higher band gap NW to the one with a smaller band gap within the bundle.

The Raman map depicted in Figure 3d results after intensity integration of the Raman peak (spectral window indicated in green in Figure 3b). It reveals stronger Raman scattering for the thinner NWs than from the thicker NWs despite their smaller material volume. We attribute this effect to resonance Raman scattering, which leads to a stronger Raman signal of thin NWs with band gap energies closer to the excitation energy. The NW bundle can also be resolved spatially in the Raman map.

Remarkably, some NWs were found to exhibit strong spatial variations of the PL energy with shifts of up to several tens of meV. In Figure 4a the energy map along a 400 nm long NW segment is depicted. Owing to the constant NW height of

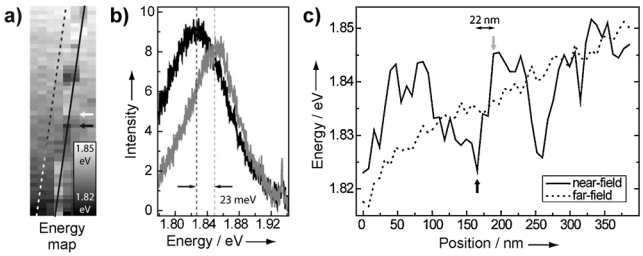

Figure 4. a) Energy map of a 400 nm long NW segment with constant diameter (8 nm) revealing substantial energy shifts at nanoscale distances. b) Spectra recorded at two positions separated by about 23 nm as marked by the arrows in (a) and (c). c) PL energy profiles measured along the NW with and without the near-field contribution as marked in (a).

(8 ± 0.5) nm (determined from topography) significant diameter-related band gap variations can be excluded. The spectra shown in Figure 4b were measured at positions separated by only 23 nm (marked in Figure 4a and c by arrows). The PL energy difference is about 22 meV, revealing energy gradients of up to 1 meV nm^{-1}. The shifts in the PL energy can most likely be attributed to crystal phase variations (WZ–ZB).

In summary, we found that the optical properties of CdSe NWs can vary significantly on the nanoscale leading to strong spatial fluctuations in both PL intensities and energies. A detailed optical characterization of these structures thus requires a sub-diffraction limit imaging technique with spectral resolution. TENOM and atomic-resolution structural data obtained by HRTEM could be combined with theoretical calculations to predict the electronic energy landscape along single NWs.

Experimental Section

The setup consists of a confocal microscope combined with a near-field (NF) probe kept in constant distance to the sample surface by a shear-force feed-back mechanism. A He–Ne laser operating at

632.8 nm is used which is converted into a radially polarized donut mode and focused onto the sample by a high numeric aperture (NA) objective. The optical response is detected either by an avalanche photo diode after spectral filtering or by a cooled charge-coupled device after passing a spectrograph. Electrochemically etched gold tips with tip radii smaller than 15 nm are used as NF probes. CdSe NWs were grown by a solution–liquid–solid method.[3,14,15]

Received: July 25, 2011
Published online: October 13, 2011

Keywords: luminescence · nanomaterials · Raman spectroscopy · semiconductors · TENOM

[1] A. J. Baca, J.-H. Ahn, Y. Sun, M. A. Meitl, E. Menard, H.-S. Kim, W. M. Choi, D.-H. Kim, Y. Huang, J. A. Rogers, *Angew. Chem.* **2008**, *120*, 5606 – 5624; *Angew. Chem. Int. Ed.* **2008**, *47*, 5524 – 5542.
[2] Y. Li, F. Qian, J. Xiang, C. M. Lieber, *Mater. Today* **2006**, *9*, 18 – 27.
[3] M. Kuno, *Phys. Chem. Chem. Phys.* **2008**, *10*, 620 – 639.
[4] H. Yu, J. Li, R. A. Loomis, P. C. Gibbons, Wang, W. E. Buhro, *J. Am. Chem. Soc.* **2003**, *125*, 16168 – 16169.
[5] J. Li, Wang, *Nano Lett.* **2003**, *3*, 1357 – 1363.
[6] V. Protasenko, K. Hull, M. Kuno, *Adv. Mater.* **2005**, *17*, 2942 – 2949.
[7] A. M. Mintairov, J. Herzog, M. Kuno, J. L. Merz, *Phys. Status Solidi B* **2010**, *247*, 1416 – 1419.
[8] E. Yoskovitz, G. Menagen, A. Sitt, E. Lachman, U. Banin, *Nano Lett.* **2010**, *10*, 3068 – 3072.
[9] L. F. Zagonel, S. Mazzucco, M. Tencé, K. March, R. Bernard, B. Laslier, G. Jacopin, M. Tchernycheva, L. Rigutti, F. H. Julien, R. Songmuang, M. Kociak, *Nano Lett.* **2011**, *11*, 568 – 573.
[10] S. Berweger, C. C. Neacsu, Y. Mao, H. Zhou, S. S. Wong, M. B. Raschke, *Nat. Nanotechnol.* **2009**, *4*, 496 – 499.
[11] A. Hartschuh, *Angew. Chem.* **2008**, *120*, 8298 – 8312; *Angew. Chem. Int. Ed.* **2008**, *47*, 8178 – 8191.
[12] L. Manna, D. J. Milliron, A. Meisel, E. C. Scher, A. P. Alivisatos, *Nat. Mater.* **2003**, *2*, 382 – 385.
[13] R. Venugopal, P. Lin, Y. Chen, *J. Phys. Chem. B* **2006**, *110*, 11691 – 11696.
[14] J. W. Grebinski, K. L. Hull, J. Zhang, T. H. Kosel, M. Kuno, *Chem. Mater.* **2004**, *16*, 5260 – 5272.
[15] Z. Li, O. Kurtulus, N. Fu, Z. Wang, A. Kornowski, U. Pietsch, A. Mews, *Adv. Funct. Mater.* **2009**, *19*, 3650 – 3661.

